四、剛性鋪面之結構評估與回算

Readings: Training Course - Module 2C

◎Structural Evaluation

Nondestructive Deflection Testing (NDT)
Equipments, Concepts, and Procedures

◎ Introduction

※Factors to be considered:

Existing distress, structural components, NDT

※Existing distress (caused primarily by traffic loadings):

AC - alligator cracking > 10%
rutting > 1/2 in.
JPCP - cracked slabs > 10%
JRCP - deter. trans. cracks > 850 ft/lane-mile
deteriorated joints > 50%
CRCP - punchouts & patches > 10/lane-mile
steel ruptures > 10/lane-mile

※Material tests:

pavement types, thickness, conditions of different layers

※NDT: most reliable; detailed deflection studies to ascertain causes of distress, to locate inadequate support or voids, to determine load transfer efficiency at joints and cracks

◎Deflection Measurement

stronger pavement => lower deflection
weaker pavement => higher deflection

◎Types of NDT Equipments:

Static deflection, Automated beam deflection, Steady-state dynamic deflection, Impulse deflection

※Static Deflection Device:

1. Benkelman Beam: Figure 5
   Need to make sure front supports are not within deflection basin
2. Plate Bearing
3. Curvature Meter

※Automated Beam Deflection Device:

1. La Croix Deflectograph
2. California Traveling Deflectometer

Technical Problems:

1. Reference point may be in the basin
2. Inadequately represent moving wheel load
3. cannot easily be used to determine load transfer across a joint or crack

※Steady-State Dynamic Deflection Device (穩態動力撓度儀)：

1. Dynaflect 動力撓度儀 - 台灣省公路局
2. Road Rater, Model 2000, 道路評審儀- 高速公路局
3. Cox Device
4. FHWA Cox Van (Thumper)

＊基本特性：

1. Static pre-load
2. Static-state sinusoidal vibration,

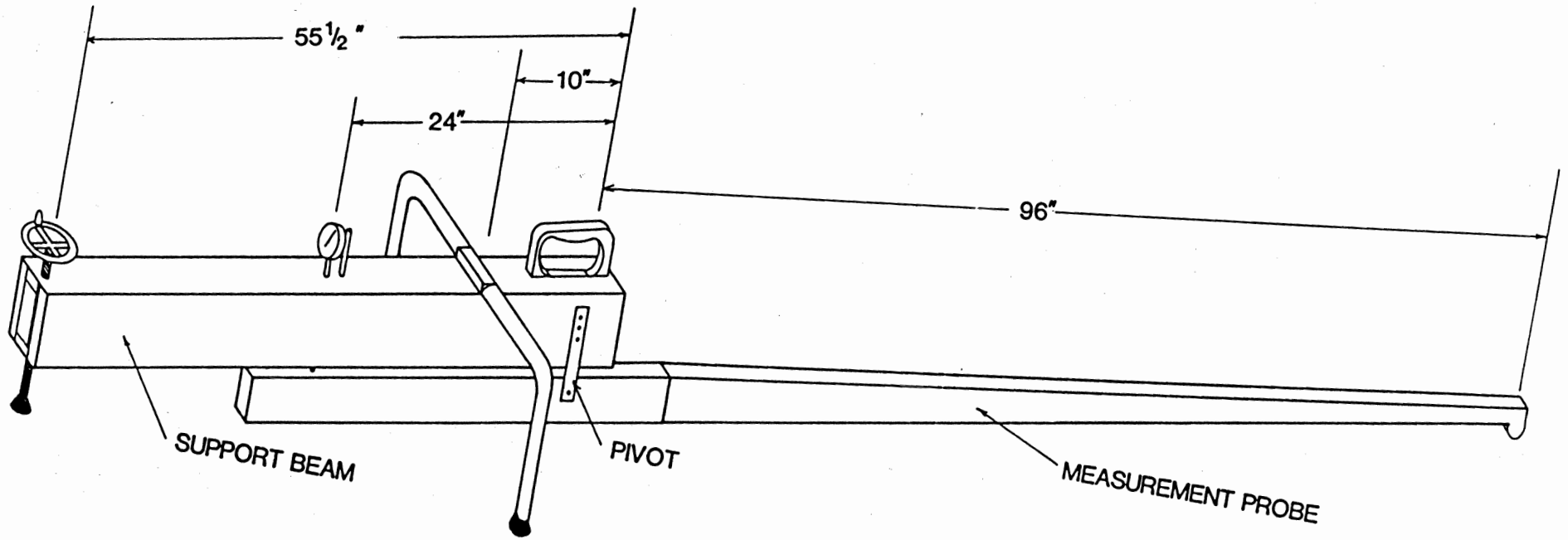

Figure 5. Sketch of Basic Components of Benkelman Beam.

dynamic force generator
3. Peak-to-peak dynamic force < 2 * static force

* Dynaflect 動力撓度儀：
1. One of the first commercially available devices
2. Static load: 2,000~2,100 pounds
3. Limitation: 6 mph, up to 1,000 pounds peak-to-peak fixed frequency

* Road Rater：Series 400B, 2000(國內),2008
1. Peak-to-peak loading 1,000-8,000 lbs
2. Load frequency: 5-70 cycles/sec
3. Technical limitation: limited load levels for lighter models, heavy static preload for heavier devices

※ Impulse Deflection Device:
1. Resulting deflection closely simulates deflection caused by a moving wheel load (Note: static preloading may change paving materials' stress states (stress-sensitivity))
2. Pre-load = 8~18% of the max. impulse load 9,000 - 24,000 lbs (Figure 7)

* Dynatest Falling Weight Deflectometer:
1. Model 8000 is the most widely used FWD device in the U.S.
2. loading plate diameter 11.8 in. (30 cm)
3. varying drop heights & weights 1,500 - 24,000 lbs

4. up to 7 sensors

* KUAB FWD:
    1. Two-mass falling weight system
    2. Smoother rise of the force pulse
    3. Dynamic force 2,698 - 35,000 lbs

* Phonix FWD:
    1. Dynamic force 2,248 - 11,240 lbs

※ Summary Characteristics of NDT Devices:
See Figure 4 or Table 9.1 (Hudson)

◎Factors Influencing Deflections

※ Loading Factors:

1. Impulse deflection equipment most closely simulates the deflection
2. Load-deflection relationship is not linear (Figure 8)
3. Recommendation: Use NDT produces loads approximate to those of heavy truck loads
4. "Correction" between different devices (static deflection > dynamic deflection) (Figure 9)
5. Special cautions and difficulties (stress-sensitive for static pre-load) (Figure 10)

※ Pavement Factors:

Distressed areas, wheel paths, joints, corners, voids, random variations, etc. (Figure 12)

Table 9.1 Characteristics of Nondestructive Deflection Testing Devices [Hudson 87a]

Device Name	Type of Unit	Loading Principle	Loading System	Static Load, lb.	Dynamic Force, lbf.	Load Transmitted by	Deflection Measuring Device	Method of Recording Data	Available in USA
Benkelman Beam	Manual Operation	Rolling Wheel	Loaded Truck	(a)	N/A	Truck Wheels	Dial Gauge	Manual	Yes
California Traveling Deflectometer	Self-Contained Automated	Rolling Wheel	Moving loaded truck	(a)	N/A	Truck Wheels	Deflection Transducer	Manual, Printed, or Automated	Yes
La Croix Deflectograph	Self-Contained Automated	Rolling Wheel	Moving truck loaded with blocks or water	(a)	N/A	Truck Wheels	Deflection Transducer	Manual, Printed, or Automated	No
Dynaflect	Trailer Mounted	Steady State Vibratory, Frequency 8 Hz	Counter rotated masses	2,100	1,000	Two 16" dia. Urethane Coated Steel Wheels	5 Geophones	Manual, Printed, or Automated	Yes
Model 400 B Road Rater	Trailer Mounted (b)	Vibratory Frequency 6–60 Hz	Hydraulic Actuated Masses	2,400	200–3,000	Two 4" by 7" Pads with 5.5" Center Gap (c)	4 Geophones	Manual, Printed, or Automated	Yes
Model 2000 Road Rater	Trailer Mounted	Vibratory Frequency 6–60 Hz	Hydraulic Actuated Masses	3,500	200–5,500	Circular Plate 18" dia. (d)	4 Geophones	Manual, Printed, or Automated	Yes
Model 2008 Road Rater	Trailer Mounted	Vibratory Frequency 5–80 Hz	Hydraulic Actuated Masses	7,500	500–9,000	Circular Plate 18" dia. (d)	4 Geophones	Manual, Printed, or Automated	Yes
KUAB 50 FWD	Trailer Mounted	Impact	Two Dropping Mass System	2,000	2,700–11,300	Sectionalized Circular Plate 11.8" dia. (d)	Up to 5 Seismometers	Manual, Printed, or Automated	Yes
KUAB 150 FWD	Trailer Mounted	Impact	Two Dropping Mass System	2,000	2,700–33,700	Sectionalized Circular Plate 11.8" dia. (d)	Up to 12 Seismometers	Manual, Printed, or Automated	Yes
Dynatest 8000 FWD	Trailer Mounted	Impact	Dropping Mass	2,000	1,500–27,000	Circular Plate 11.8" dia. (d)	7 Geophones	Manual, Printed, or Automated	Yes
Dynatest 800 FWD	Trailer Mounted	Impact	Dropping Mass	2,000	6,500–19,000	Circular Plate 11.8" dia. (d)	7 Geophones	Manual, Printed, or Automated	Yes
Phonix ML 10000 FWD	Trailer Mounted	Impact	Dropping Mass	1,900	2,300–23,000	Circular Plate 11.8" dia. (d)	3 or 6 Geophones		Yes
CRSTP Curvimeter	Self-Contained	Rolling Wheel	Moving truck loaded with steel pellets	(a) or variable	N/A	Truck Wheels		Automated	Yes

a. 18,000 lbs single axle truck
b. Earlier versions were mounted on vehicles
c. Circular plates are available
d. Plates of other dimensions are available

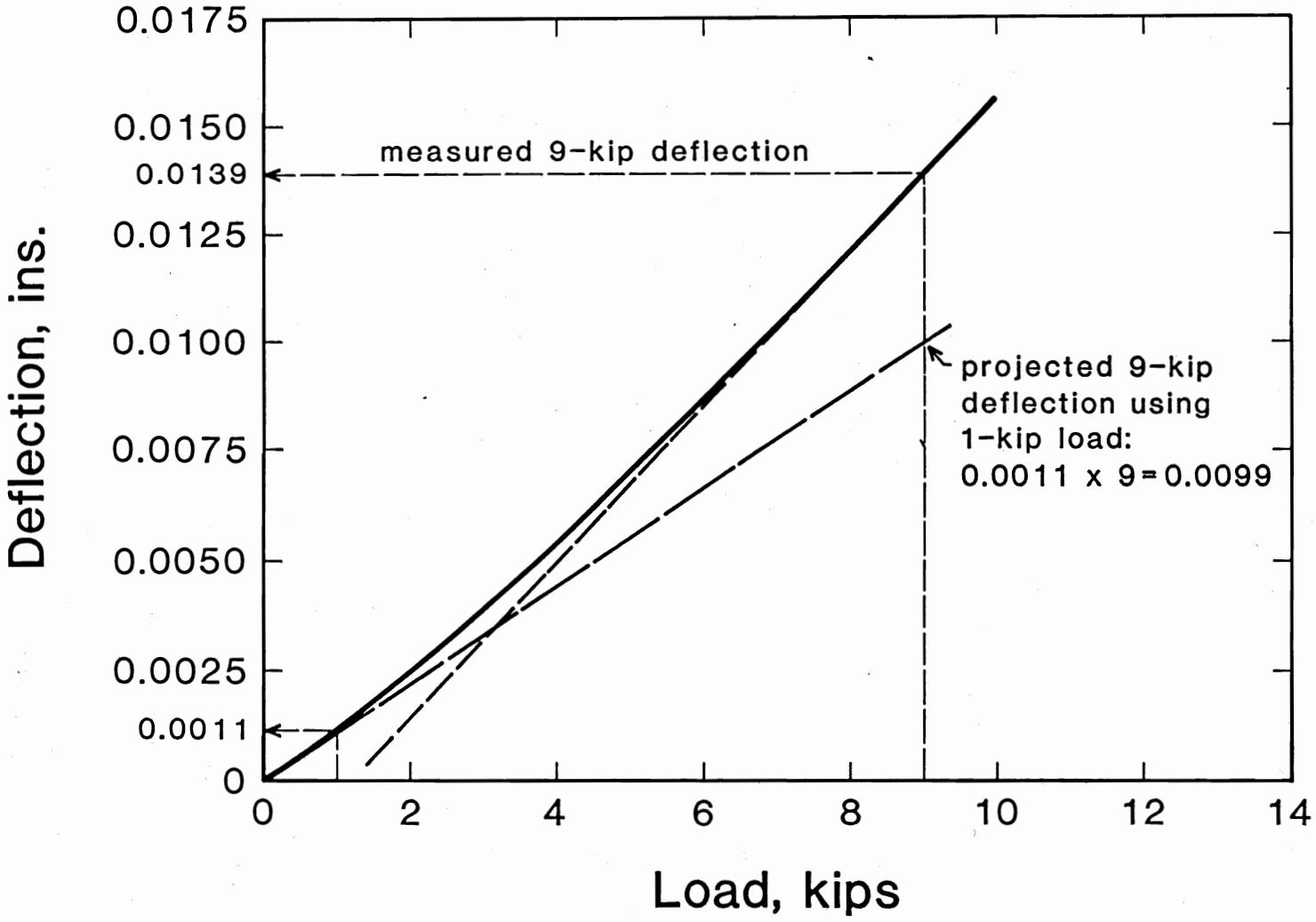

Figure 8. Deflection vs. Peak-to-Peak Dynamic Load.

Note: Nonlinear shape and poor projection of 9-kip deflection from 1-kip loading. This illustrates the danger of projecting deflections from heavy loads using very light loads.

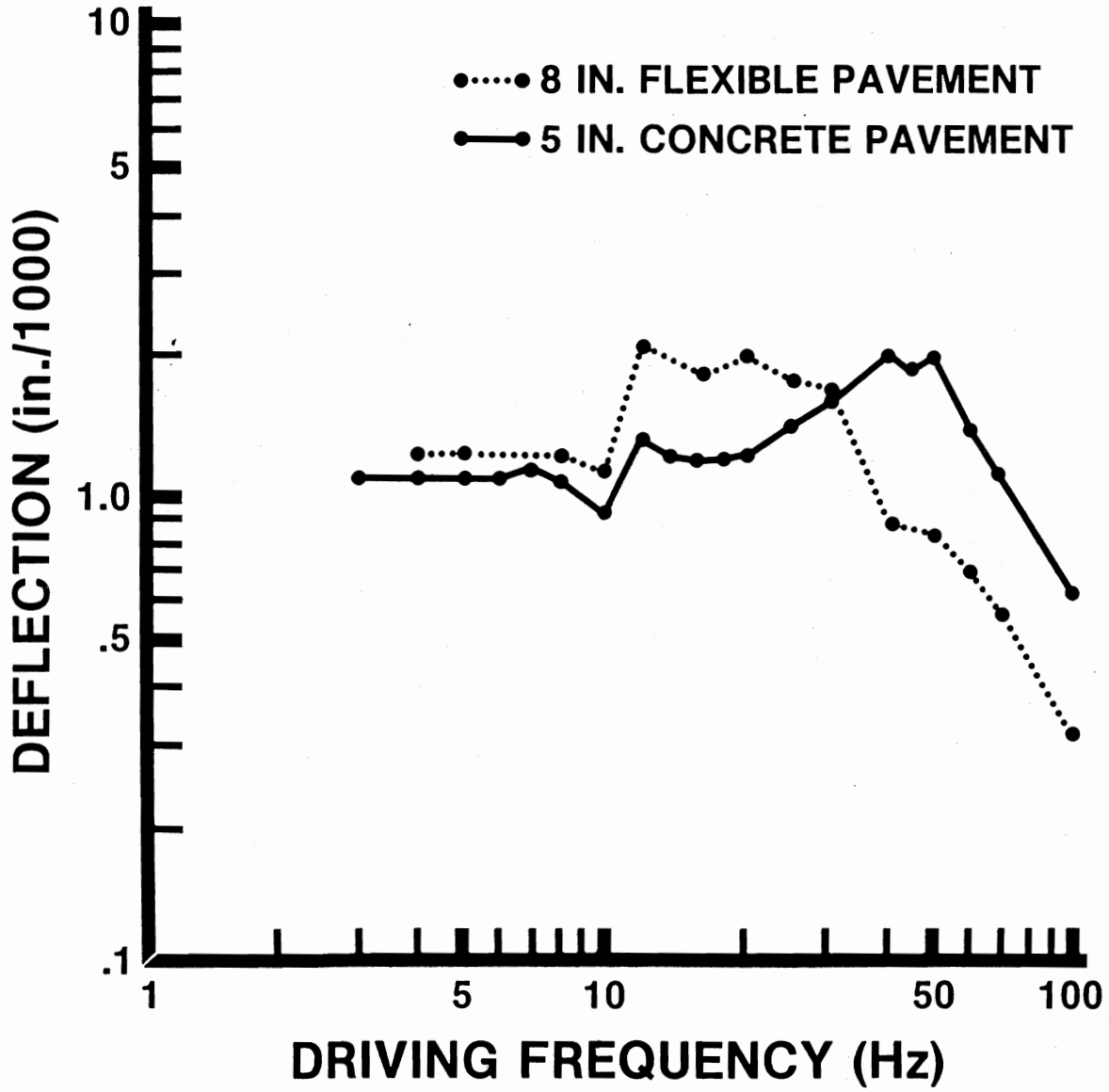

Figure 10. Variation of Deflection with Frequency of Loading (2).

※Climatic Factors:

1. Higher AC surfacing temperature => higher deflection (Figure 13)
2. Higher PCC temperature => tighter joints & cracks => higher load transfer efficiency (LTE) => lower deflection
3. Thermal gradients:
   $\Delta T>0$ (day-time) => lower deflection
   $\Delta T<0$ (night-time) => higher edge or corner deflection
4. Seasonal variation: (Figure 14)

➔ Time of the day & season of the year

➔ Standard temperature (70 °F) & season, equivalent deflection based on locally developed procedures

◎Conducting NDT Field Survey

1. Temperature measurement
2. Deflection along the project length
3. More detailed intensive deflection if necessary

◎Special Test Procedures

※Deflection Profile: shape of deflection basin

1. Dynaflect Max. Deflection (DMD)
2. Surface Curvature Index (SCI=D1-D2)
3. Base Curvature Index (BCI=D1-D3)

※Utah Overlay Design Procedure (Figure 18)

※Load Transfer Efficiency (LTE) (Figure 19)

◎Interpretation of Structural Testing Data

Uniformity of the project

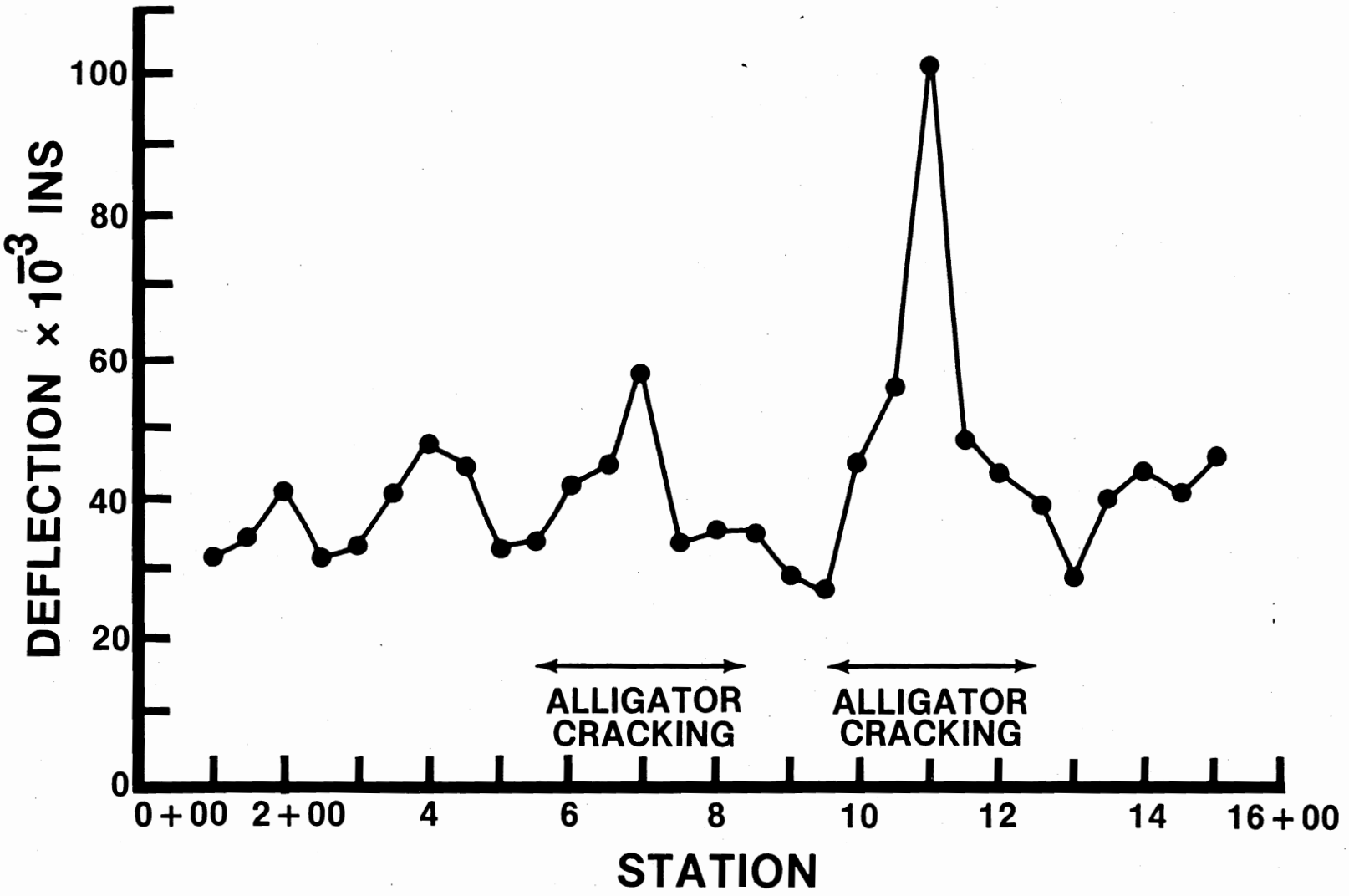

Figure 12. Effect of Alligator Cracking on Deflections in Asphalt Concrete Pavements (9 Kip Load).

Figure 13. Influence of Temperature on Asphalt Pavement Deflection (4).

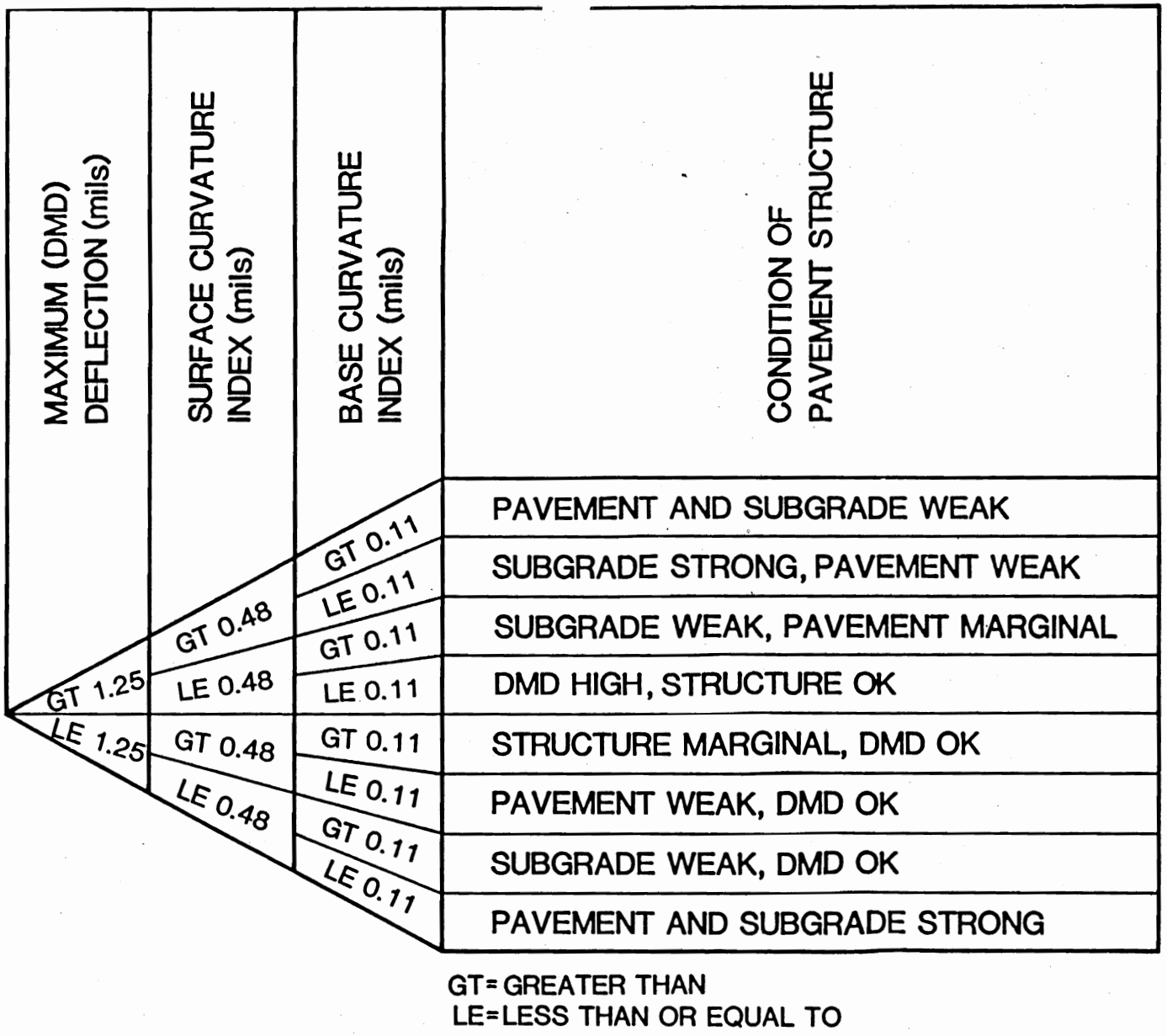

Figure 18. Use of Deflection Basin Parameters to Analyze Pavement Structural Layers, from Utah Overlay Design Procedure.

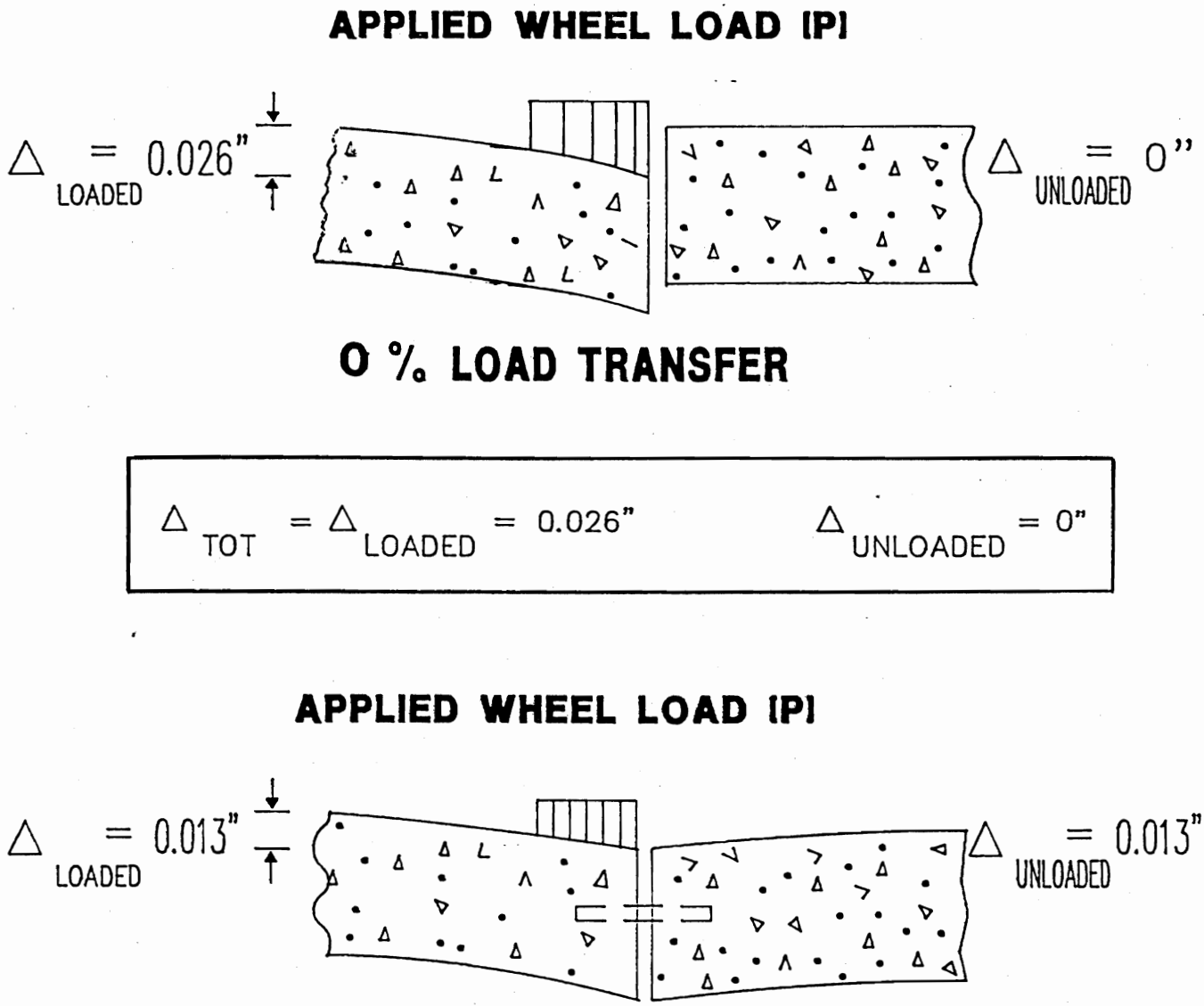

Figure 19. Effect of Load Transfer.

C 剛性鋪面之回算

C.1 剛性鋪面回算之介紹

資料來源：

林炳森、李泰明、吳元廷、鄒譽名，“路面評審儀應用於剛性路面之回算法”，中華民國第八屆鋪面工程學術研討會論文輯，台北國際會議中心，中原大學，中華民國八十四年十二月六日至八日。

C.2 剛性鋪面回算之封閉型解法

資料來源：

Hall, K. T., “Performance, Evaluation, and Rehabilitation of Asphalt-Overlaid Concrete Pavements,” Ph.D. Thesis, University of Illinois, Urbana, Illinois, 1991, pp. 88-104.

◎常用的非破壞性試驗儀器：

動力撓度儀(Dynaflect)

路面評審儀(Road Rater)

衝擊荷重撓度儀(Falling Weight Deflectometer)

◎回算法之分類：

反覆計算法：BISDEF, CHEVDEF, WESDEF, ELSDEF

資料庫處理法：COMDEF, MODULUS

◎反覆計算法尚待解決之問題：

彈性模數值的解可能不唯一、回算結果受輸入資料範圍的影響甚巨、反覆運算的過程不僅耗費時間甚至可能不收斂

◎Westergaard (1926)與Losberg (1960)之理論解

1. 路基土壤爲緊密液體

$$w^* = \frac{\delta k \ell^2}{P} = \frac{\delta D}{P\ell^2} = f(\frac{a}{\ell}, \frac{r}{\ell})$$

$$\ell = \ell_k = \sqrt[4]{\frac{Eh^3}{12(1-\mu^2)k}}$$

$$D = \frac{Eh^3}{12(1-\mu^2)}$$

2. 路基土壤爲彈性固體

$$w^* = \frac{\delta C \ell}{2P} = \frac{\delta D}{P\ell^2} = f(\frac{a}{\ell}, \frac{r}{\ell})$$

$$\ell = \ell_e = \sqrt[3]{\frac{Eh^3(1-\mu_s^2)}{6(1-\mu^2)E_s}}$$

$$C = \frac{E_s}{(1-\mu_s^2)}$$

其中:

w^* = 版之無因次撓度值

D = 版之撓屈勁度,$[L^4]$

C = 路基土壤常數,$[FL^{-2}]$

r = 與載重中心點之徑向距離,$[L]$

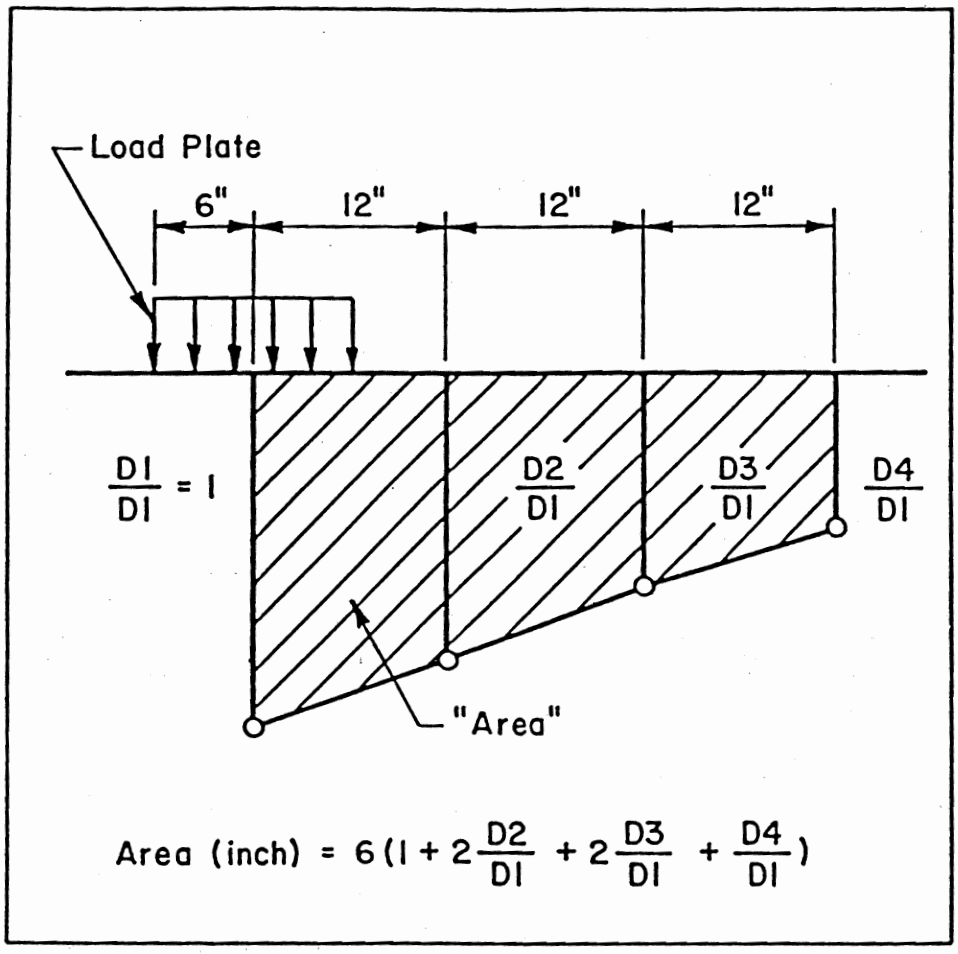

Figure 25. Calculation of Deflection Basin "AREA"

◎撓度盤區域面積(AREA) 的方法

Hoffman和Thompson (1981)對AREA的定義如下：(AREA的單位為長度，最大值為36) (Figure 25)

$$AREA = 6*\left[1+2\left(\frac{d_{12}}{d_0}\right)+2\left(\frac{d_{24}}{d_0}\right)+\left(\frac{d_{36}}{d_0}\right)\right]$$

其中:

d_0 = 載重中心點正下方之最大撓度值,[L]

d_i = 離載重中心點 i 處(12, 24, 36英吋)之撓度值,[L]

ERES 和Foxworthy (1985)依據不同之混凝土彈性模數值(E)、路基反力模數值(k)、與版厚度(h)，建立一系列之最大撓度值與AREA之關係圖，並利用內插圖解法反算出該系統之E值與k值。(Figure 26)

Homework #2:

Please perform a series of ILLI-SLAB runs to construct a graph of curves for backcalculation in a similar way.

◎ 回算之封閉型解與ILLI-BACK程式

Ioannides (1990)並指出在固定的載重半徑與量測固定徑向距離之撓度值情況下，AREA與相對勁度半徑有唯一的關係，並建立ILLI-BACK程式。

Hall (1991)進而利用FORTRAN之IMSL副程式庫，對於該封閉型解(含多種特殊之貝索函數Bessel Functions)直接積分，並利用SAS統計軟體推導出AREA與相對勁度半徑之迴歸關係式：(Fig. 4.1-4.2)

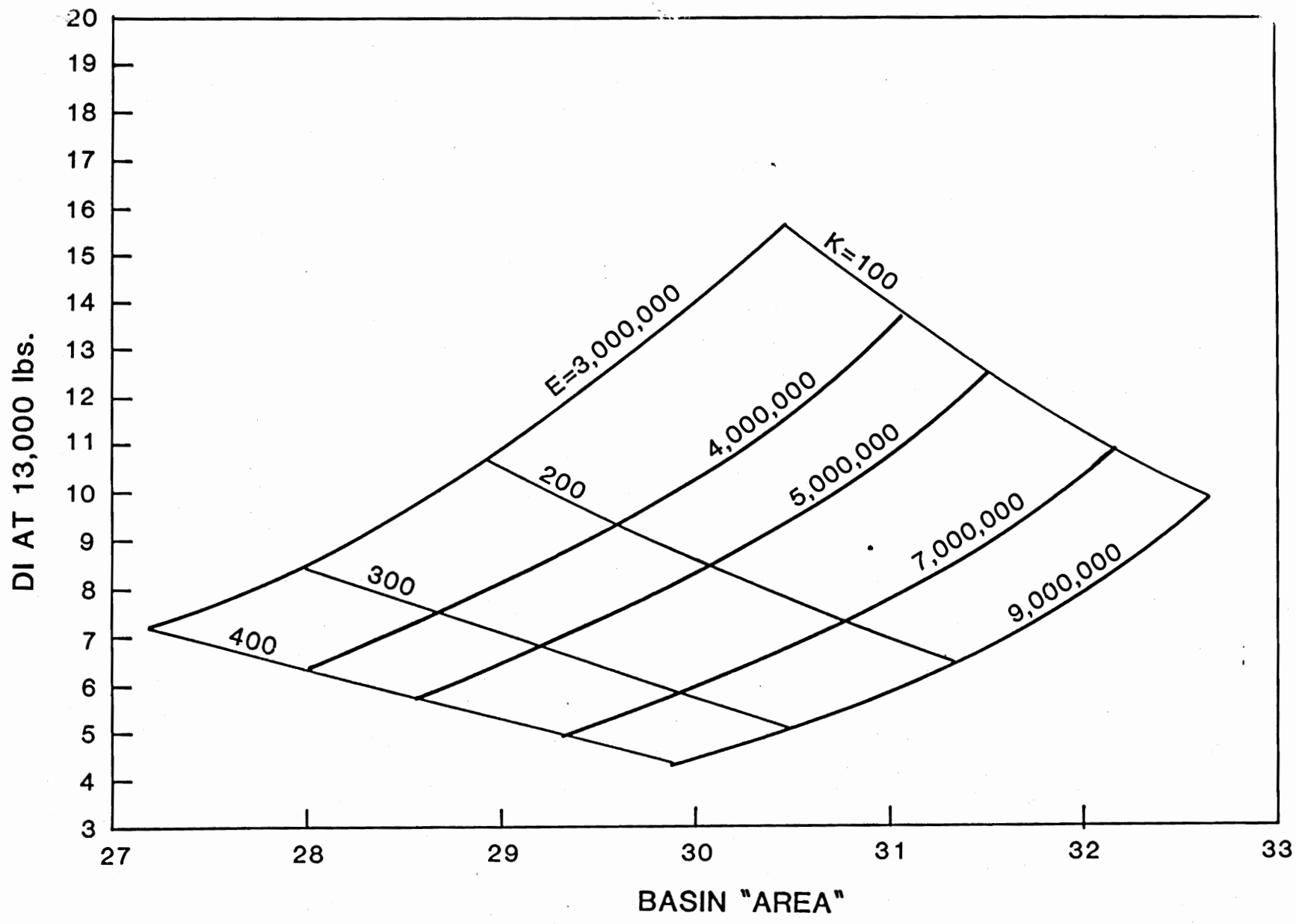

Figure 26. Nomograph Developed for Concrete Pavement Modulus Value Backcalculation Example.

$$\ell_k = \left[\frac{\ln\left(\frac{36 - AREA}{1812.279133}\right)}{-2.559340} \right]^{4.387009}$$

$$\ell_e = \left[\frac{\ln\left(\frac{36 - AREA}{4521.676303}\right)}{-3.645555} \right]^{5.334281}$$

因此，由上述迴歸方程式即可利用已知AREA值推算出其相對勁度半徑值。再利用Westergaard內部撓度方程式之重新排序，即可由已知最大撓度值求解路基土壤之反力模數值：

$$k = \frac{P}{8 d_0 \ell_k^2} \left\{ 1 + \frac{1}{2\pi} \left[\ln\left(\frac{a}{2\ell_k}\right) + \gamma - 1.25 \right] \left(\frac{a}{\ell_k}\right)^2 \right\}$$

或利用Losberg內部撓度方程式之重新排序，即可由已知最大撓度值求解路基土壤之彈性模數值：

$$E_s = \frac{2P\left(1-\mu_s^2\right)}{d_0 \ell_e} \left[0.19245 - 0.0272\left(\frac{a}{\ell_e}\right)^2 + 0.0199\left(\frac{a}{\ell_e}\right)^2 \ln\left(\frac{a}{\ell_e}\right) \right]$$

混凝土版之彈性模數值也可因此由版與路基土壤之相對勁度半徑公式直接求解而得。

Homework #4

Please use Hall's equation and the graph constructed in previous Homework #2 to compare both backcalculation procedures using the same example inputs.

(Additional Reading: Huang's Text Book P.456-459.)

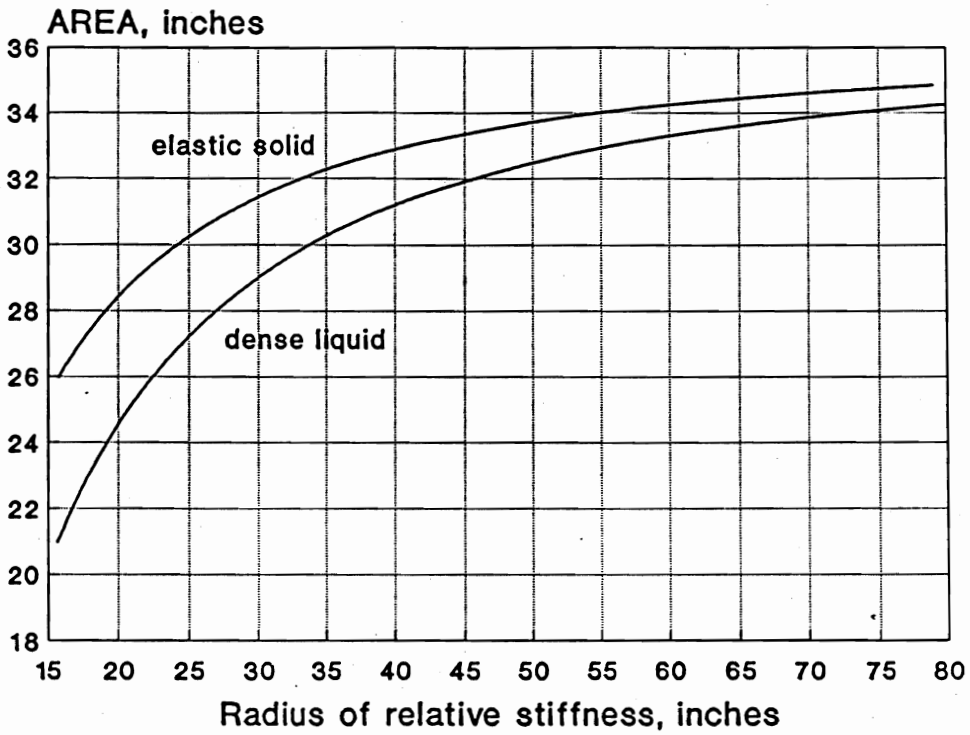

Figure 4.1 Deflection AREA versus radius of relative stiffness.

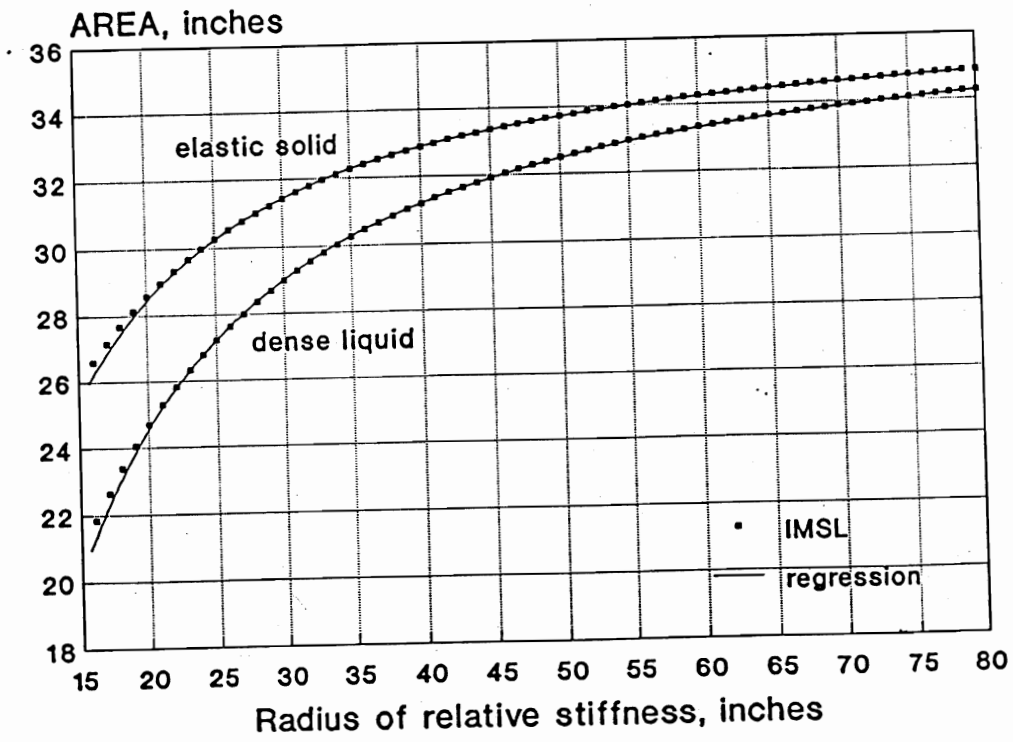

Figure 4.2 Comparison of AREA versus ℓ values and regression models.

2. 路基土壤爲彈性固體(Elastic Solid Foundation)

$$w^* = \frac{\delta C\ell}{2P} = \frac{\delta D}{P\ell^2} = f(\frac{a}{\ell}, \frac{r}{\ell})$$

$$\ell = \ell_e = \sqrt[3]{\frac{Eh^3(1-\mu_s^2)}{6(1-\mu^2)E_s}}$$

$$C = \frac{E_s}{(1-\mu_s^2)}$$

其中:

w^* = 版之無因次撓度值

δ = 版之撓度值,[L]

D = 版之撓屈勁度,[L^4]

C = 路基土壤常數,[FL^{-2}]

P = 單輪載重,[F]

h = 版之厚度,[L]

k = 路基反力模數,[FL^{-3}]

a = 載重半徑,[L]

r = 與載重中心點之徑向距離,[L]

ℓ = 版與路基之相對勁度半徑,[L]

E, E_S = 混凝土版與路基土壤之彈性模數,[FL^{-2}]

μ, μ_s = 版與路基土壤之柏松比

Hoffman和Thompson (1981)並建議採用計算撓度盤區域面積(AREA)的方法，以回算出二層混凝土鋪面系統之彈性模數值與路基反力模數值。AREA的定義如下：(需

周家蓓、張德文、賴登明、林家吉、黃偉慶、汪立威、梁履坦，林志棟、倪志寬等。再者，李英豪(本計畫主持人)、李英明、陳建桓，在執行　貴會專題計畫：「運用因次分析的方法對混凝土鋪面角隅應力之理論評估」(編號NSC83-0410-E032-009和NSC84-2211-E032-022)時，亦針對「由面層撓度值回算鋪面彈性模數的初步研究」提出可行之改進方向。

在國外方面，近十多年來鋪面非破壞性檢測與彈性模數回算一直是學術研究極爲熱門的話題，各相關電腦程式亦相繼建立。然而，誠如筆者在「由面層撓度值回算鋪面彈性模數的初步研究」報告中所述，目前仍存在一些基本的問題尚待解決，以致學術研究的成果仍然無法與工程實務界密切配合。此外，國外對「接縫式混凝土鋪面彈性模數回算」之研究亦是極弱的一環。

從最早Westergaard (1926)根據無限版長及完全路基支承的假設，所得出鋪面結構之理論反應解開始，Losberg (1960)並提出混凝土版在受到載重下之無因次撓度盤(Nondimensional Deflection Basins)公式與圖解：

1. 路基土壤爲緊密液體(Dense Liquid Foundation)

$$w^* = \frac{\delta k \ell^2}{P} = \frac{\delta D}{P\ell^2} = f(\frac{a}{\ell}, \frac{r}{\ell})$$

$$\ell = \ell_k = \sqrt[4]{\frac{Eh^3}{12(1-\mu^2)k}}$$

$$D = \frac{Eh^3}{12(1-\mu^2)}$$

特別注意的是AREA的單位爲長度，最大值爲36。)

$$AREA = 6*\left[1+2\left(\frac{d_{12}}{d_0}\right)+2\left(\frac{d_{24}}{d_0}\right)+\left(\frac{d_{36}}{d_0}\right)\right]$$

其中:

d_0 = 載重中心點正下方之最大撓度值,[L]

d_i = 離載重中心點 i 處(12, 24, 36英吋)之撓度值,[L]

ERES Concultants, Inc. (1982)和Foxworthy (1985)因此利用數百次以上的有限元素法程式之執行，依據不同之混凝土彈性模數值、路基反力模數值、與版厚度，以建立一系列之最大撓度值與AREA之關係圖，進而利用內插圖解法反算出該二層系統之彈性模數值與路基反力模數值。唯內插圖解法過程繁複，精確度不足，且不利於一般鋪面回算所需之大量批次運算爲其主要之缺點。

Ioannides (1990)並指出在固定的載重半徑與量測固定徑向距離之撓度值情況下，撓度盤之區域面積AREA與版與路基土壤之相對勁度半徑有唯一的關係。Ioannides也因此編寫一FORTRAN程式(ILLI-BACK)，以協助各彈性模數值與路基反力模數值之回算。唯該封閉型解(Closed-Form Solution)僅適用於Westergaard (1926)所假設之無限版尺寸與完全路基支承。對於能更實際地模擬鋪面版有限的尺寸、及可能因線性溫差而產生局部喪失路基支承之情形，則仍有待於有限元素法程式的進一步分析。再者，ILLI-BACK程式之求解過程仍不利於大量之批次運算，且該程式爲著作權法保護之軟體，無法隨意取得。

Hall (1991)進而利用IMSL之FORTRAN副程式庫，對於前述之封閉型解(含多種特殊之貝索函數Bessel Functions)直接積分，並利用SAS統計軟體推導出撓度盤之區域面積AREA與版與路基土壤之相對勁度半徑之迴歸關係式：

$$\ell_k = \left[\frac{\ln\left(\frac{36 - AREA}{1812.279133}\right)}{-2.559340} \right]^{4.387009}$$

$$\ell_e = \left[\frac{\ln\left(\frac{36 - AREA}{4521.676303}\right)}{-3.645555} \right]^{5.334281}$$

因此，由上述迴歸方程式即可利用已知AREA值推算出版與路基土壤之相對勁度半徑值。再利用Westergaard內部撓度方程式之重新排序，即可由已知最大撓度值求解路基土壤之反力模數值：

$$k = \frac{P}{8 d_0 \ell_k^2} \left\{ 1 + \frac{1}{2\pi} \left[\ln\left(\frac{a}{2\ell_k}\right) + \gamma - 1.25 \right] \left(\frac{a}{\ell_k}\right)^2 \right\}$$

或利用Losberg內部撓度方程式之重新排序，即可由已知最大撓度值求解路基土壤之彈性模數值：

$$E_s = \frac{2P\left(1-\mu_s^2\right)}{d_0 \ell_e} \left[0.19245 - 0.0272 \left(\frac{a}{\ell_e}\right)^2 + 0.0199 \left(\frac{a}{\ell_e}\right)^2 \ln\left(\frac{a}{\ell_e}\right) \right]$$

混凝土版之彈性模數值也可因此由版與路基土壤之相對勁度半徑公式直接求解而得。

Crovetti (1994)進一步指出非破壞性撓度試驗之荷重盤位置(版之內部、邊界、或角隅)亦會影響回算之結果。Crovetti 並針對邊界與角隅荷重之情況，利用Westergaard與Losberg相關撓度公式，建議與上述回算鋪面各層彈性模數相似之推算過程。此外，混凝土版之有限尺寸、相臨混凝土版之荷重傳遞效應、及可能因線性溫差而產生局部喪失路基支承之效應，均有賴於有限元素法程式的再進一步分析。

在深入文獻回顧後發現，其中與本計畫最相關之研究有A.M. Ioannides, K. T.

◎ C.3 ILLI-SLAB程式之使用手冊

資料來源：

Korovesis, G. T., "Analysis of Slab-on-Grade Pavement Systems Subjected to Wheel and Temperature Loadings," Ph.D. Thesis, University of Illinois, Urbana, Illinois, 1990, pp. 305-334.

※ ILLISLABS程式Input 檔之範例：

分析之狀態以雙軸對稱之中央荷重。在Load = 9000 lbs，a = 5.9 in.固定下，胎壓為常數等於82.3 psi，荷重區域之長度為c = 10.46 in.，因分析之狀態為雙軸對稱。所以取1/2 c = 5.23 in.。

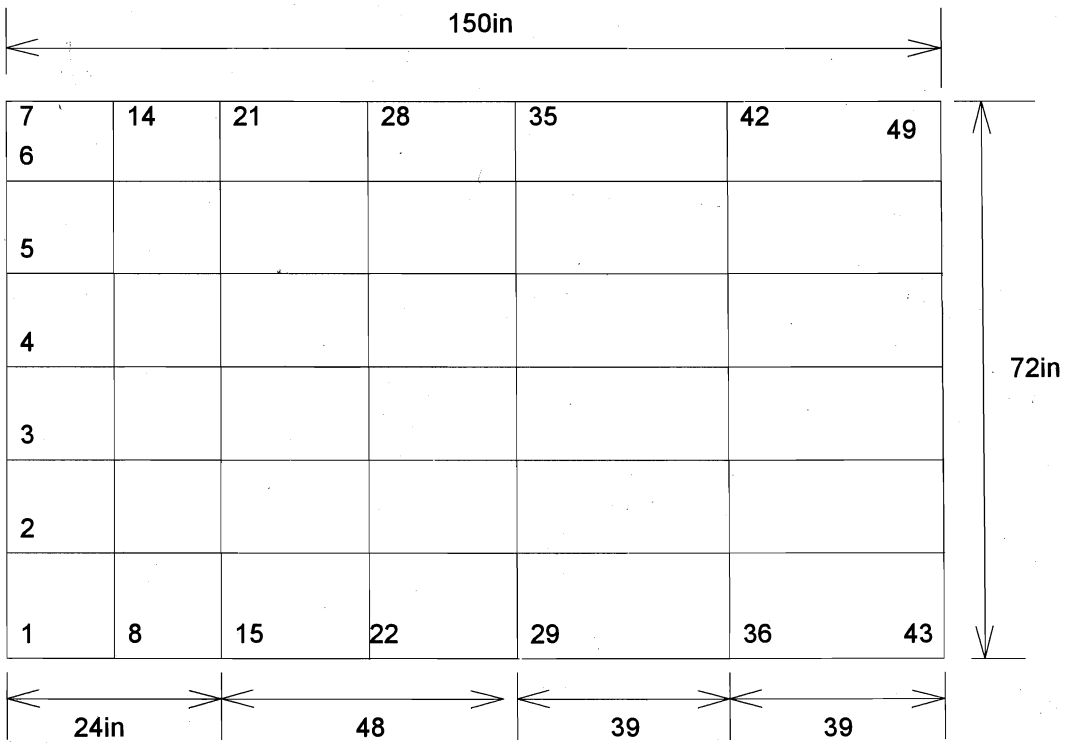

```
1
Slab Size h=10 K=100 E=3E6 infinite slabs p=9000lbs a=5.9
    1    3    0    0
    7
    7
    1    0   100.000
    6    1 0.05 0.05    1
000000  40
       0.0       12.0       24.0       48.0       72.0      111.0      150.0
       0.0       12.0       24.0       36.0       48.0       60.0       72.0
      10.0   3.00E+06       0.15      0.136       16.0   6.88E-06
     82.30        0.0       5.23        0.0       5.23
```

◎ C.4 對ILLI-SLAB使用者之建議

資料來源：

Ioannides, A. M., "Analysis of Slab-on-Grade for a Variety of Loading and Support Conditions," Ph.D. Thesis, University of Illinois, Urbana, Illinois, 1984, pp. 187-188.

1. At least one node at the expected max. response location
2. 2a/h ≤ 0.8, finer mesh extends 2 times the loaded area, gradually increase the mesh size
3. "Winkler" model use option IST=6 is better than IST=7
4. Keep 2a/2b ≅ 1 extending to 2 times of radius of the loaded area; keep 2a/2b < 4~5 elsewhere

※ ILLI-SLAB for PC Version

(a) DOS conventional memory at least ≥ 550 KB (approximately)

(b) Keep at least 17 MB of hard disk space (depends on the size of the problem defined)

(c) ILSB89.EXE < INPUT.FIL > OUTPUT.FIL

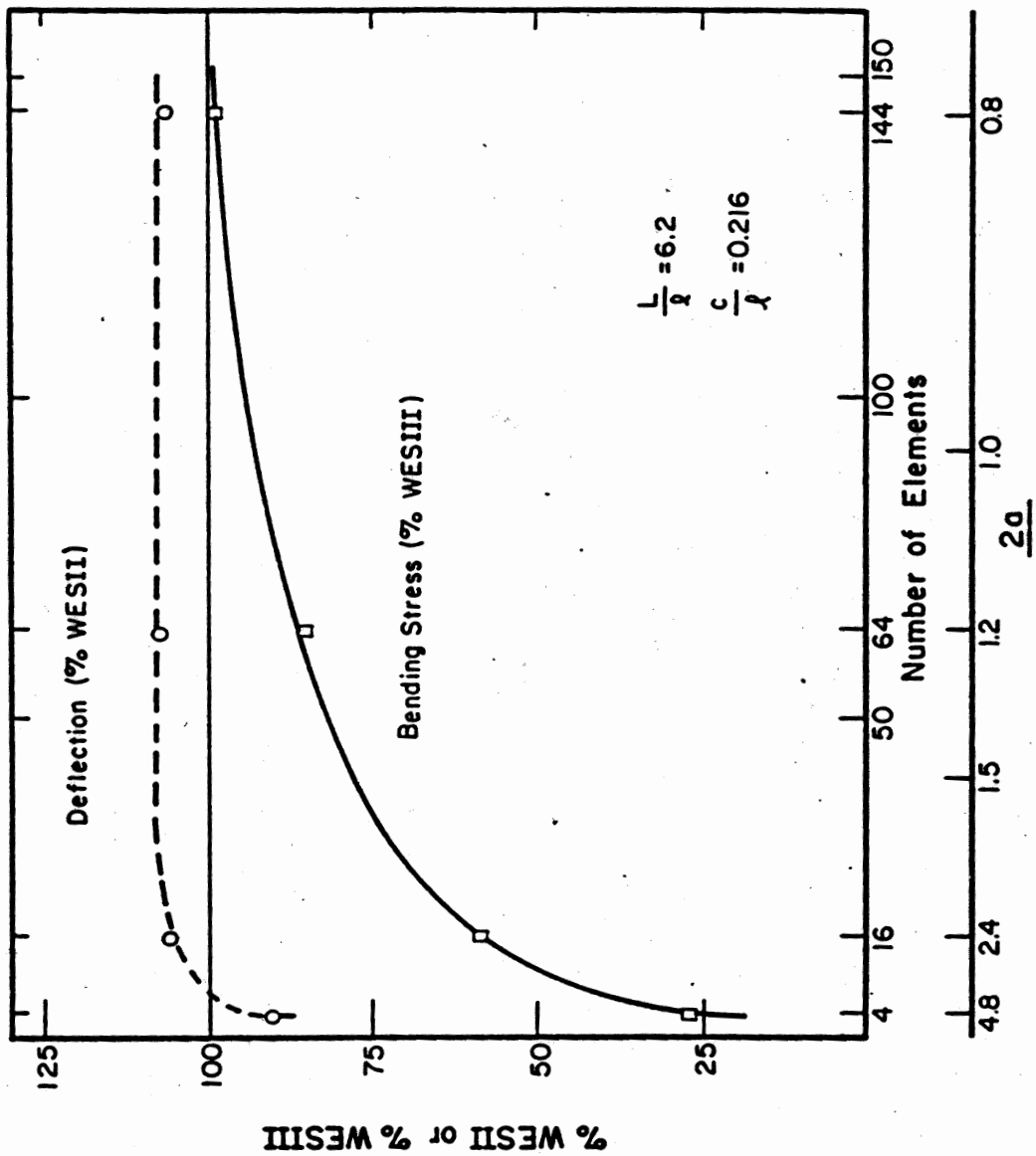

Fig. 5.6 Effect of Mesh Fineness (Interior Loading)

一、假設有一剛性鋪面版，其相關基本性質與荷重資料如下：Slab size(長 × 寬)= 12ft × 12ft，Slab thickness=10in.，Slab Ec =4,000,000psi，μ=0.15，P = 9,000lbs，Loaded area =10 in. × 10 in.，k =100 pci，Interior / Edge / Corner loading。請利用 ILLI-SLAB 有限元素程式，求解其最大應力與撓度值，並與 Westergaard 理論解公式相比較，另請與 ILLISTRS 程式所得之應力相比較。

答：

1. 利用 ILLI-SLAB 有限元素程式，求解其最大應力與撓度值：

(1) ILLI-SLAB 中央應力分析：假設應力狀態為對稱 X 軸與 Y 軸，在 X 方向分 19 個結點與 Y 方向分 22 個結點。

輸入值：

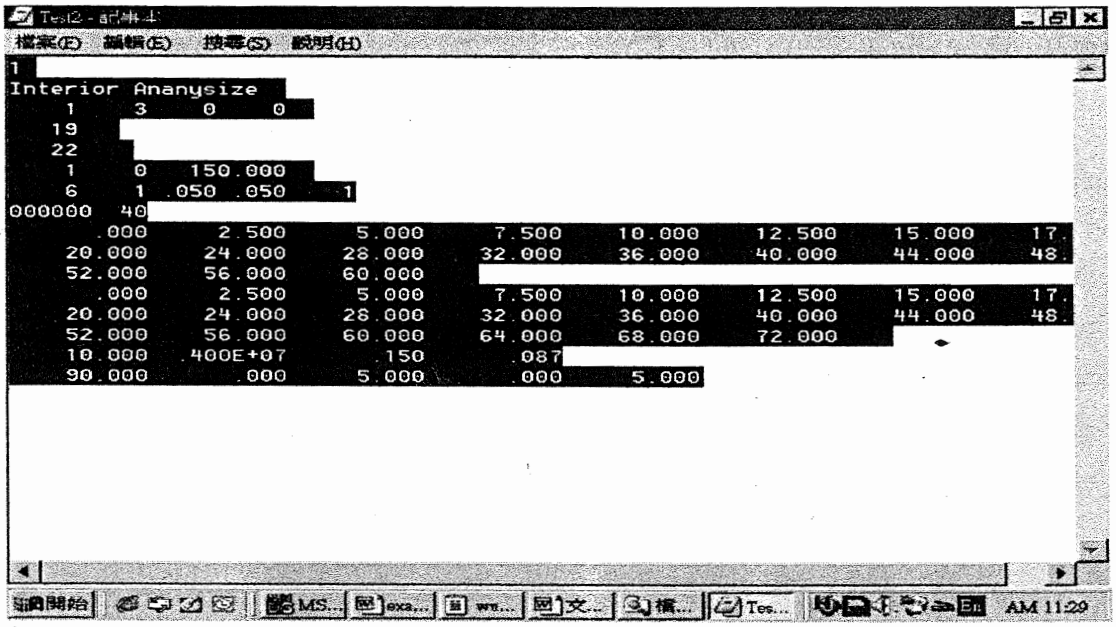

輸出值：

MAXIMUM OR MINIMUM VALUES OF (COMPRESSION IS POSITIVE)

DEFLECTION = .006156 AT NODE 1 AND .000000 AT NODE 0

SUBGRADE STRESS = .923 AT NODE 1

RANGE OF X-STRESS AT BOTTOM OF LAYER 1: FROM -125.061 AT NODE 1 TO 2.492 AT NODE 331

RANGE OF Y-STRESS AT BOTTOM OF LAYER 1: FROM -133.665 AT NODE 1 TO 1.751 AT NODE 19

RANGE OF MINOR PRINC. STRESS BOT. LAYER 1: FROM -133.665 AT NODE 1 TO .000 AT NODE 418

RANGE OF MAJOR PRINC. STRESS BOT. LAYER 1: FROM -125.061 AT NODE 1 TO 2.492 AT NODE 331

NOTE:- X-STRESS TOP = - (X-STRESS BOTTOM)

Y-STRESS TOP = - (Y-STRESS BOTTOM)

MINOR PRINC. STRESS TOP = - (MAJOR PRINC. STRESS BOTTOM)

MINOR PRINC. STRESS BOTTOM = - (MAJOR PRINC. STRESS TOP)

SUM OF REACTION FORCES = 2249.29

SUM OF EXTERNAL FORCES AND SELF-WEIGHT (IF ANY) = 2250.00

Stop - Program terminated.

(2) ILLI-SLAB 邊緣應力分析：假設應力狀態為對稱 Y 軸，在 X 方向分 19 個結點與 Y 方向分 40 個結點。

輸入值：

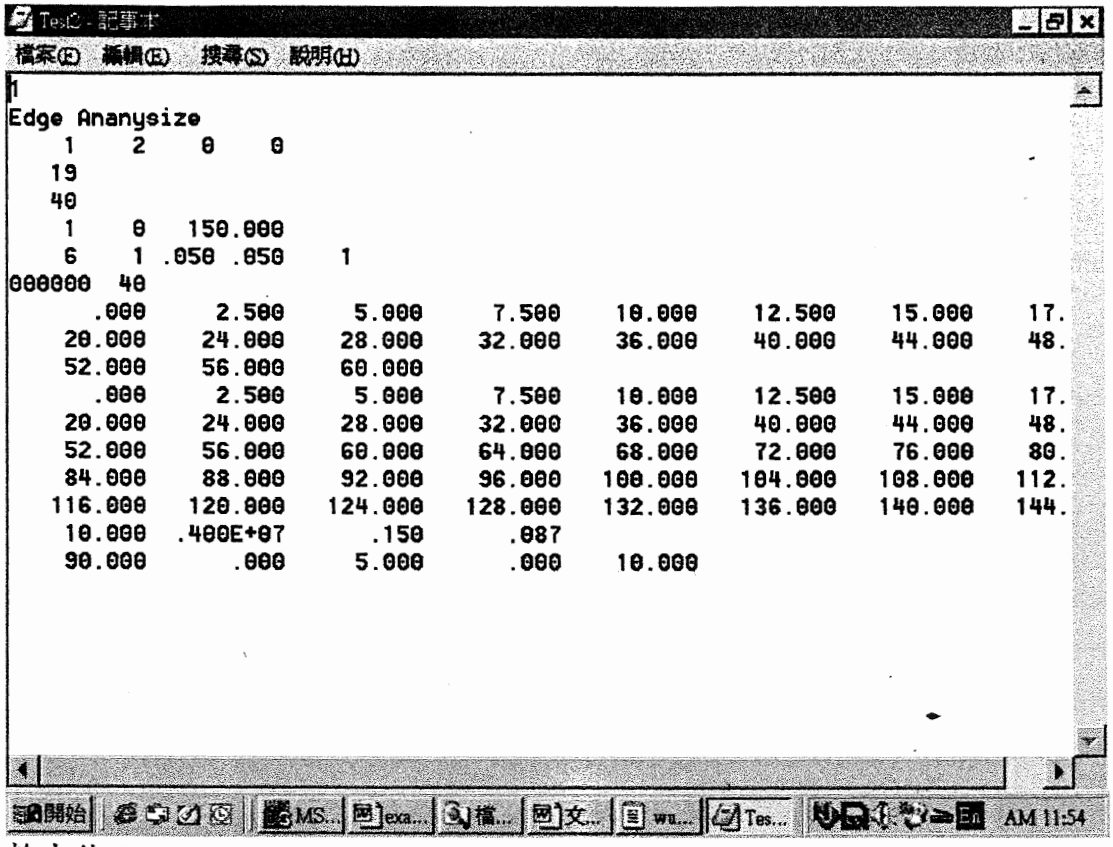

輸出值：

MAXIMUM OR MINIMUM VALUES OF (COMPRESSION IS POSITIVE):

DEFLECTION = .020284 AT NODE 1 AND -.003768 AT NODE 760

SUBGRADE STRESS = 3.043 AT NODE 1

RANGE OF X-STRESS AT BOTTOM OF LAYER 1: FROM -233.401 AT NODE 1 TO 18.691 AT NODE 601

RANGE OF Y-STRESS AT BOTTOM OF LAYER 1: FROM -30.065 AT NODE 3 TO 71.531 AT NODE 14

RANGE OF MINOR PRINC. STRESS BOT. LAYER 1: FROM -233.401 AT NODE 1 TO .000 AT NODE 760

RANGE OF MAJOR PRINC. STRESS BOT. LAYER 1: FROM -30.065 AT NODE 3 TO 71.531 AT NODE 14

NOTE:- X-STRESS TOP = - (X-STRESS BOTTOM)

Y-STRESS TOP = - (Y-STRESS BOTTOM)

MINOR PRINC. STRESS TOP = - (MAJOR PRINC. STRESS BOTTOM)

MINOR PRINC. STRESS BOTTOM = - (MAJOR PRINC. STRESS TOP)

SUM OF REACTION FORCES = 4501.73

SUM OF EXTERNAL FORCES AND SELF-WEIGHT (IF ANY) = 4500.00

Stop - Program terminated.

(3) ILLI-SLAB 角隅分析：假設應力狀態無對稱，在 X 方向分 34 個結點與 Y 方向分 40 個結點。

輸入值：

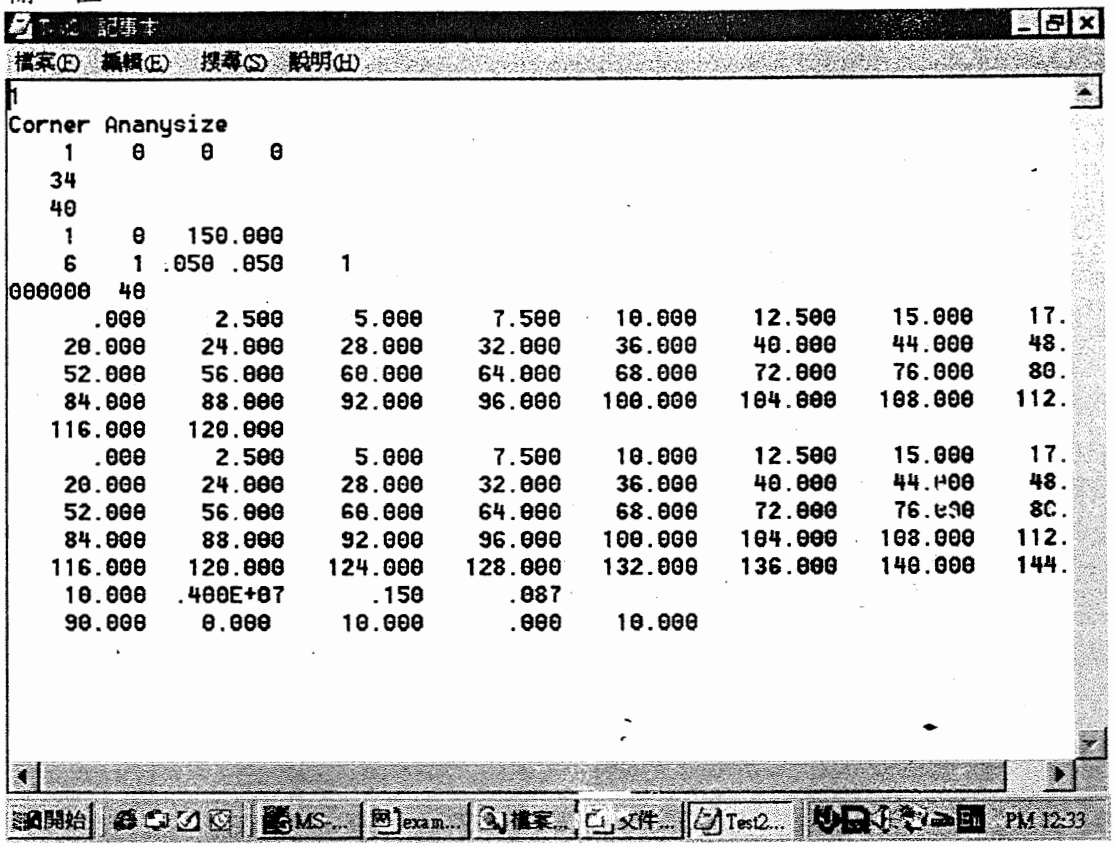

輸出值：

MAXIMUM OR MINIMUM VALUES OF (COMPRESSION IS POSITIVE):

DEFLECTION = .043454 AT NODE 1 AND -.006437 AT NODE 1360

SUBGRADE STRESS = 6.518 AT NODE 1

RANGE OF X-STRESS AT BOTTOM OF LAYER 1: FROM -85.206 AT NODE 81 TO 116.103 AT NODE 561

RANGE OF Y-STRESS AT BOTTOM OF LAYER 1: FROM -84.960 AT NODE 3 TO 122.956 AT NODE 16

RANGE OF MINOR PRINC. STRESS BOT. LAYER 1: FROM -139.425 AT NODE 124 TO 3.380 AT NODE 543

RANGE OF MAJOR PRINC. STRESS BOT. LAYER 1: FROM .000 AT NODE 1360 TO 172.678 AT NODE 53

NOTE:- X-STRESS TOP = - (X-STRESS BOTTOM)

Y-STRESS TOP = - (Y-STRESS BOTTOM)

MINOR PRINC. STRESS TOP = - (MAJOR PRINC. STRESS BOTTOM)

MINOR PRINC. STRESS BOTTOM = - (MAJOR PRINC. STRESS TOP)

SUM OF REACTION FORCES = 9008.2

SUM OF EXTERNAL FORCES AND SELF-WEIGHT (IF ANY) = 9000.00

Stop - Program terminated.

Normally three iterations of the program can produce a set of modulus values that yield a deflection basin within an accuracy of 3%. Iterations will cease when the absolute sum of the percent differences between computed and measured deflections or the predicted change in modulus values becomes less than 10%.

ILL-BACK Program

In contrast to the optimization programs that require the input of seed moduli, ILL-BACK can determine the moduli of rigid pavement directly without the use of a search routine (Ioannides et al., 1989). The program can be applied to a concrete slab on a liquid or solid foundation with a circular load at the interior. The deflections at four sensors with distances of 0, 12, 24, and 36 in. (0, 305, 610, and 914 mm) from the center are measured and the moduli of the slab and the foundation can be back-calculated.

For liquid foundations, Westergaard's equation for deflection at the center of loading was shown in Eq. 4.21 and can be expressed as

$$d_0 = \frac{w_0 k \ell^2}{P} = f\left(\frac{a}{\ell}\right) \tag{9.41}$$

in which d_0 is the normalized deflection under the center of loading and f is a function of a/ℓ. For a given contact radius a, d_0 is a function of the radius of relative stiffness ℓ only. Similar equations can be obtained for sensor i at a given distance from the center:

$$d_i = \frac{w_i k \ell^2}{P} = f_i(\ell) \tag{9.42}$$

in which i can be 0, 1, 2, or 3. For a given ℓ, the normalized deflection d_i can be determined from theory. If the deflection w_i at any sensor i is measured, the modulus of subgrade reaction k can be computed by Eq. 9.42. Now the crucial question is how to determine ℓ. Once ℓ is known, the deflection measured by any one of the sensors can be used to determine k. A comparison of these k values can provide an evaluation of the agreement between theory and field measurements.

If two deflections, w_0 and w_1, are measured, then from Eq. 9.42

$$d_0 = \frac{w_0 k \ell^2}{P} = f_0(\ell) \tag{9.43a}$$

$$d_1 = \frac{w_1 k \ell^2}{P} = f_1(\ell) \tag{9.43b}$$

Dividing Eq. 9.43b by 9.43a gives

$$\frac{d_1}{d_0} = \frac{w_1}{w_0} = \frac{f_1}{f_0} = f(\ell) \tag{9.44}$$

Equation 9.44 indicates that ℓ can be determined from the deflection ratio, w_1/w_0. If four sensors are used, it is more reliable to use the average deflection of all four sensors, as indicated by the area of deflection basin:

$$\text{AREA} = 6\left[1 + 2\left(\frac{w_1}{w_0}\right) + 2\left(\frac{w_2}{w_0}\right) + \left(\frac{w_3}{w_0}\right)\right] \tag{9.45}$$

Note that Eq. 9.45 is based on a sensor spacing of 12 in. (305 mm) and the unit of AREA is in inches.

Figure 9.39 shows the relationship between AREA and ℓ for both liquid and solid foundations, as obtained from theory. The solid curves are based on a circular load with a radius of 5.9 in. (150 mm) and the broken curves on a concentrated load with a radius of zero. It can be seen that the effect of radius on the AREA versus ℓ relationship is not very significant.

After ℓ is determined from Figure 9.39, the normalized deflection d_i can be determined from Figure 9.40 for liquid foundations and Figure 9.41 for solid foundations. For liquid foundations, k can be determined from Eq. 9.42:

$$k = \frac{P d_i}{\ell^2 w_i} \tag{9.46}$$

It can be shown that E_f for solid foundation can be determined by (Ioannides, 1990)

$$E_f = \frac{2(1 - \nu_f^2)\, P d_i}{\ell w_i} \tag{9.47}$$

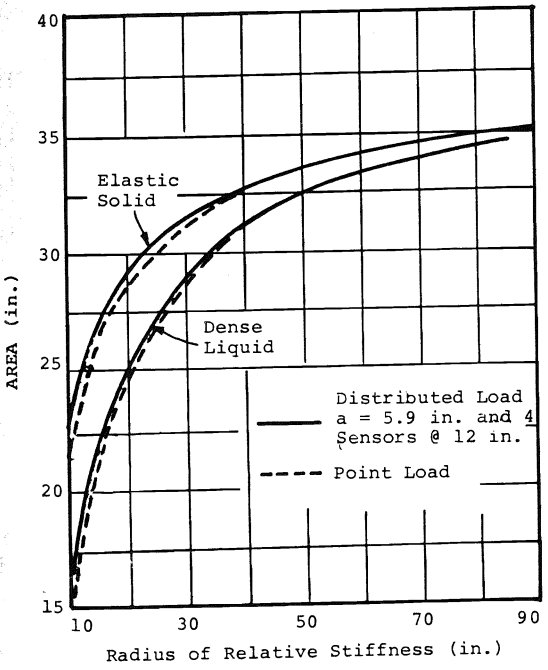

Figure 9.39 Relationship between AREA and ℓ (1 in. = 25.4 mm). (After Ioannides et al. (1989).)

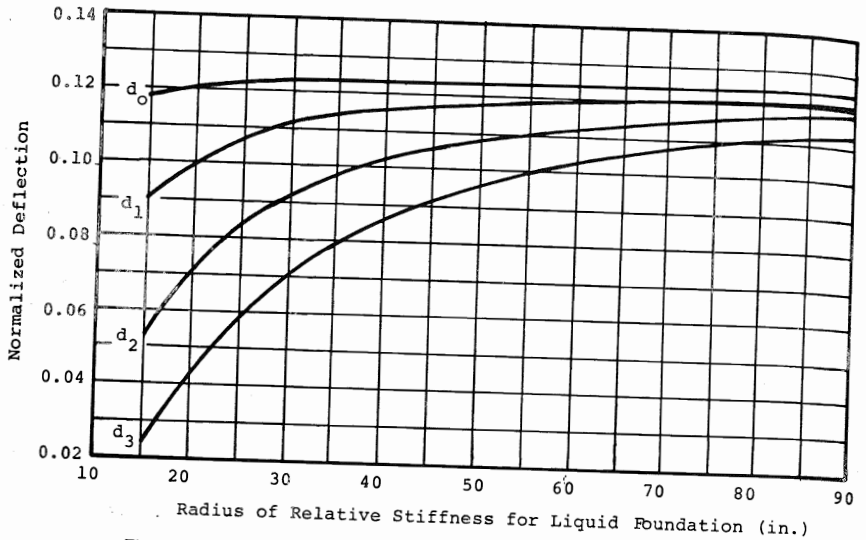

Figure 9.40 Relationship between normalized deflections and ℓ for liquid foundations (1 in. = 25.4 mm). (After Ioannides et al. (1989).)

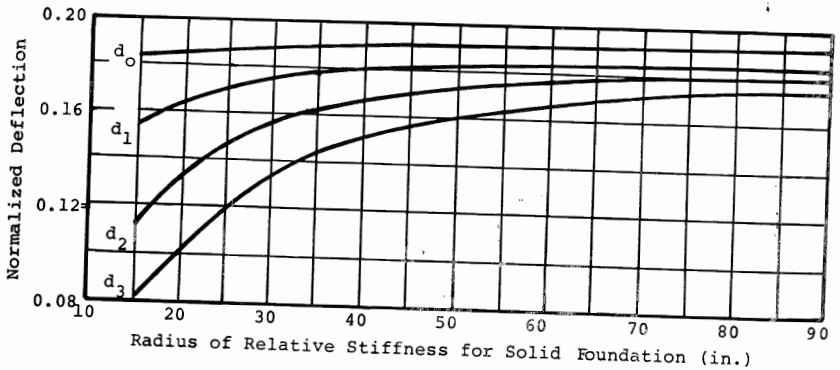

Figure 9.41 Relationship between normalized deflections and ℓ for solid foundations (1 in. = 25.4 mm). (After Ioannides et al. (1989).)

The radius of relative stiffness for liquid foundation is defined by Eq. 4.10, and that for solid foundation is defined by Eq. 5.38. These equations can be used to compute the elastic modulus of concrete E_c if the slab thickness h is known or vice versa.

The elastic modulus of concrete E_c for liquid foundations can be computed from Eq. 4.10:

$$E_c = \frac{12(1 - \nu_c^2)\, k\ell^4}{h^3} \tag{9.48}$$

For solid foundations, from Eq. 5.38

$$E_c = \frac{6(1 - \nu_c^2)\, E_f \ell^3}{(1 - \nu_f^2)\, h^3} \tag{9.49}$$

The procedure for back-calculating the moduli of concrete and foundation can be summarized as follows:

1. Measure deflections, w_0, w_1, w_2, and w_3.
2. Compute AREA by Eq. 9.45.
3. Determine ℓ from Figure 9.39.
4. For liquid foundations, determine the normalized deflection from Figure 9.40 and compute k by Eq. 9.46. Four k values, one for each sensor, are obtained and their average is taken. For solid foundations, determine the normalized deflection from Figure 9.41 and compute E_f by Eq. 9.47. The average of the four values is taken as E_f.
5. Based on the average k or E_f, compute E_c by Eq. 9.48 or 9.49.

Example 9.4

A FWD test was conducted on a 10-in. (254-mm) concrete pavement. The radius of the loaded plate is 5.9 in. (300 mm) and the recorded load is 7792 lb (34.7 kN). Sensors were located at 0, 12, 24, and 36 in. (0, 305, 610, and 914 mm) and the corresponding deflections recorded are 0.0030, 0.0028, 0.0024, and 0.0021 in. (0.076, 0.071, 0.061, and 0.053 mm). It is assumed that the concrete has a Poisson ratio of 0.15. (a) If the subgrade is considered as a liquid foundation, determine k and E_c. (b) If the subgrade is considered as a solid foundation with a Poisson ratio of 0.45, determine E_f and E_c.

Solution: From Eq. 9.45, AREA = 6[1 + 2(2.8/3) + 2(2.4/3) + 2.1/3] = 31.0 in. (787 mm). From Figure 9.39, ℓ = 39 in. (991 mm) for liquid foundation and 28 in. (711 mm) for solid foundation.

(a) For a liquid foundation, from Figure 9.40, $d_0 = 0.123$, $d_1 = 0.115$, $d_2 = 0.102$, and $d_3 = 0.085$. From Eq. 9.46 and based on w_0 and d_0, $k = 7792 \times 0.123/[(39)^2 \times 0.0030] = 210$ pci (57.0 MN/m^3). The k values based on the other three sensors are 210, 218, and 207 pci (57.0, 59.1, and 56.2 MN/m^3). The mean of the four k values is 211 pci (57.3 kN/m^3). From Eq. 9.48, $E_c = 12[1 - (0.15)^2] \times 211 \times (39)^4/(10)^3 = 5.7 \times 10^6$ psi (39.3 GPa).

(b) For a solid foundation, from Figure 9.41, $d_0 = 0.188$, $d_1 = 0.174$, $d_2 = 0.152$, and $d_3 = 0.128$. From Eq. 9.47 and based on w_0 and d_0, $E_f = 2[1 - (0.45)^2] \times 7792 \times 0.188/(28 \times 0.0030) = 27{,}816$ psi (192 MPa). Values of E_f based on the other three sensors are 27,583, 28,111, and 27,055 psi (190, 194, and 187 MPa). The mean E_f is 27,641 psi (191 MPa). From Eq. 9.49, $E_c = 6 \times [1 - (0.15)^2] \times 27{,}641 \times (28)^3/\{[1 - (0.45)^2] \times (10)^3\} = 4.5 \times 10^6$ psi. Because of the incompatibility between liquid and solid foundations, it is expected that the elastic modulus of concrete based on a solid foundation is somewhat different from that based on a liquid foundation.